

RESEARCH

Open Access



Circ-PSMB1 knockdown inhibits the pyroptosis of ox-LDL treated human aortic cells via the miR-624-3p/ASC axis

Yupu Zhou¹ and Yongchuan Guo^{1*}

Abstract

Background Atherosclerosis (AS) is a cardiovascular disease that is caused by a variety of factors, including hypertension, diabetes, hyperlipidaemia and smoking. Circular RNAs (circRNAs) have been reported to participate in the progression of AS. Here, we investigated the mechanism by which circ-proteasome 20 S subunit beta 1 (PSMB1) participates in AS.

Methods HAECs were stimulated with oxidized low-density lipoprotein (ox-LDL) to establish a model of AS in vitro. Cell viability was investigated with MTT assays. Western blotting and qRT-PCR were used to measure relative protein and mRNA expression. Cell pyroptosis was analysed by flow cytometry. Lactate dehydrogenase (LDH) levels were measured with a commercial kit.

Results We found that circ-PSMB1 and apoptosis-associated speck-like protein containing a CARD (ASC) were overexpressed and miR-624-3p was expressed at low levels in HAECs treated with ox-LDL. Circ-PSMB1 silencing enhanced cell viability and decreased pyroptosis, as shown by the downregulation of IL-1 β and IL-18 mRNA expression as well as NOD-like receptor thermal protein domain associated protein 3 (NLRP3) and GasderminD-N (GSDMD-N) protein expression. In addition, the miR-624-3p inhibitor neutralized the effects of si-circ-PSMB1, and ASC overexpression neutralized the effects of the miR-624-3p mimic in ox-LDL-treated HAECs.

Conclusion This research demonstrated that circ-PSMB1 might participate in AS development through regulating the pyroptosis of HAECs via the miR-624-3p/ASC axis.

Keywords Atherosclerosis, Circ-PSMB1, Pyroptosis, miR-624-3p, ASC

*Correspondence:

Yongchuan Guo
drguoyongchuan@hotmail.com

¹Department of Vascular Surgery, Jiangjin Centre Hospital, No. 725,
Jiangzhou Avenue, Dingshan Street, Jiangjin District, Chongqing,
Chongqing 402260, China



© The Author(s) 2025. **Open Access** This article is licensed under a Creative Commons Attribution-NonCommercial-NoDerivatives 4.0 International License, which permits any non-commercial use, sharing, distribution and reproduction in any medium or format, as long as you give appropriate credit to the original author(s) and the source, provide a link to the Creative Commons licence, and indicate if you modified the licensed material. You do not have permission under this licence to share adapted material derived from this article or parts of it. The images or other third party material in this article are included in the article's Creative Commons licence, unless indicated otherwise in a credit line to the material. If material is not included in the article's Creative Commons licence and your intended use is not permitted by statutory regulation or exceeds the permitted use, you will need to obtain permission directly from the copyright holder. To view a copy of this licence, visit <http://creativecommons.org/licenses/by-nc-nd/4.0/>.

Introduction

Atherosclerosis (AS) is a cardiovascular disease that is caused by a variety of factors, including hypertension, diabetes, hyperlipidaemia and smoking [1]. Cardiovascular diseases caused by AS pose a serious threat to human health [2]. The occurrence of AS can cause vascular wall injury and inflammatory reactions, which may occur due to the apoptosis and necrosis of vascular smooth muscle cells and endothelial cells and the differentiation of macrophages [3, 4]. Emerging evidence confirmed AS was closely related to somatic mutations in stem cells [5], gut microbiome [6] and immune system disorder [7]. Additionally, AS is also a chronic disease that is characterized by lipid metabolism disorder, incomplete endothelium, monocyte/macrophage proliferation and plaque formation [8]. During the evolution of AS lesions, oxidized low-density lipoprotein (ox-LDL), a key molecule [9], binds to receptors to stimulate the differentiation of monocytes/macrophages into foam cells, which produce a large number of inflammatory factors. Therefore, the development of AS is promoted [10].

Recent studies have shown that in human AS, cell death occurs via cytolysis rather than apoptosis [11, 12]. Pyroptosis is a unique new form of cell death that depends on caspase-1 and was discovered in recent years, and it is characterized by cell lysis and the release of cytosolic contents into the extracellular space, leading to inflammation [13]. When cells are exposed to external danger signals such as bacterial toxins or viral infections, pattern recognition receptors in the host innate immune system recognize pathogen-associated molecular patterns or damage-associated molecular patterns, which work together with the adaptor molecule apoptosis-associated speck-like protein containing a CARD (ASC) to recruit pro-Caspase-1, thereby activating the inflammasome and inducing pyroptosis [14, 15]. Therefore, the expression of ASC is crucial for the occurrence of pyroptosis.

Circular RNAs (circRNAs) are special noncoding endogenous RNAs. With the continuous development of high-throughput sequencing and bioinformatics, it has been shown that a large number of circRNAs are present in the transcriptome of eukaryotic cells [16, 17]. The main difference between circRNAs and linear RNAs is that circRNAs have no 5' and 3' polyadenylate tails and form a closed circular structure via covalent bonds [18]. This special circRNA structure makes these molecules difficult to hydrolyse via exonucleases, so they are more stable than linear RNAs and exhibit evolutionary conservation [19]. CircRNAs contain miRNA response elements, which can bind to miRNAs as competitive endogenous RNAs (ceRNAs), inhibit the binding of miRNAs to mRNAs in the cytoplasm and regulate gene expression [20]. This function is called "miRNA sponge". For instance, *Circhipk3*, which is a human cell

growth regulator, acts as a molecular sponge of miRNA, directly binds to miR-124 and inhibit its expression [21]. Additionally, *CircRNA_0044073* was reported to be overexpressed in AS and to inhibit the expression of miRNA-107 through a sponge mechanism, promoting the proliferation of human vascular smooth muscle cells and vascular endothelial cells [22]. In addition to these, an increasing number of literature reports on the expression and function of different circRNAs in AS [23–25]. These studies suggest that circRNAs serve as miRNA sponges to participate in the development of AS and may be an important direction for research on AS treatment.

Here, we found a up-regulated circRNA, circ-(proteasome 20 S subunit beta 1) PSMB1, through the GEO database (GSE173719). We found that the expression level of circ-PSMB1 showed the most significant difference in AS. Additionally, the specific mechanisms of circ-PSMB1 in AS progression has not been explored. Therefore, this study established an in vitro model of AS by stimulating HAECs with ox-LDL to further analyse the potential mechanism by which circ-PSMB functions in AS progression.

Materials and methods

Clinical serum sample collection

This study enrolled 2 participants diagnosed with AS and 25 healthy individuals who underwent physical examinations at our hospital during the same period. All participants provided written informed consent in accordance with the Declaration of Helsinki. Peripheral blood samples were collected from both AS patients and healthy controls after an overnight fast (minimum 8 h). Blood was drawn using sterile venipuncture techniques into EDTA-coated tubes for plasma isolation or into serum separator tubes for serum preparation. Blood collection was performed between 7:00 AM and 9:00 AM to control for potential circadian variations. Following blood collection, samples were immediately placed on ice and transported to the laboratory for processing within 1 h. For serum preparation, blood samples were allowed to clot at room temperature for 30 min before centrifugation at $1,000 \times g$ for 15 min at 4 °C. The serum samples were stored at -80 °C.

Bioinformatic analysis

All the differentially expressed circRNAs in AS were acquired from the GEO database (GSE173719). A heatmap and volcano map of differentially expressed circRNAs in AS were generated by using the *preprocessCore* package in R software. Additionally, the target miRNAs of circ-PSMB1 were predicted using StarBase software (<https://rnasysu.com/encori/>), and the target genes of miR-624-3p were predicted using Targetscan software (https://www.targetscan.org/vert_80/).

Cell culture

Human aortic endothelial cells (HAECs) and smooth muscle cells were provided by the American Type Culture Collection (ATCC, USA). All the cells were cultured at 37 °C and 5% CO₂ in DMEM supplemented with 10% foetal bovine serum and 1% penicillin and streptomycin throughout this experiment. Next, according to previous studies [26, 27], to establish AS model in vitro, 50 µg/mL ox-LDL was added to the cells and incubated for 24 h prior to further experiments. The cells in the control group were cultured in normal DMEM for 24 h.

Cell transfection

Small interfering RNA targeting circ-PSMB1 (si-circ-PSMB1) #1 and #2 and si-nc; miR-624-3p mimic and mimic nc; inhibitor and inhibitor nc; and ASC over-expression pcDNA3.1 vector and empty vector were obtained from Genepharma (Shanghai, China). These siRNAs are selective for circ-PSMB1. HAECs were transfected with 20 µM siRNA, 50 nM mimic, 100 nM inhibitor and 0.2 µg pcDNA3.1 using a Lipofectamine 2000 kit (Invitrogen, USA), respectively. After 48 h transfection, the cells were cultured in normal medium for 24 h for the next experiments.

si-circ-PSMB1 #1: 5'-AACCAGTACTATACTGGCAAT-3'

si-circ-PSMB1 #2: 5'-ACCAGTACTATACTGGCAAT-3'

si-NC: 5'-GCAAGCTGACCCTGAAGTT-3'

miR-624-3p mimic: 5'-CACAAGGUAUUGGUAUUA-3'

miR-624-3p inhibitor: 5'-AGGUAAUACCAUACCU-3'

mimic NC: 5'-UCACAACCUCCUAGAAAGAGUAG-3'

inhibitor NC: 5'-CAGUACUUUUGUGUAGUACA-3'

RNA fluorescence in situ hybridization (FISH)

Cy3-labeled circ-PSMB1 probe was designed and synthesized by Sangon (Shanghai, China). A FISH kit (GenePharma) was used to perform FISH to assess the subcellular localization of circ-PSMB1. Briefly, cells were fixed with ethanol for 15 min and treated with TritonX-100 for 15 min. The cells were hybridized with denatured probe buffer at 37 °C overnight. After washing with SSC solution, the cells were incubated with DAPI for 20 min. The signals were observed under a confocal laser scanning microscope.

qRT-PCR

The levels of IL-1β, IL-18, circ-PSMB1, miR-624-3p and ASC were determined by qRT-PCR analysis. Briefly, RNA was isolated from the cells with TRIzol reagent

(Beyotime, Jiangsu, China). After evaluating the purity and quality, the RNAs were used to synthesize cDNA with a reverse transcription kit (BioMarker, Beijing, China). Then, qRT-PCR was performed with a BioMarker 2X SYBR Green Fast qPCR Mix kit (BioMarker). The reaction system was incubated at 42 °C for 15 min. The additional chamber temperature incubation step is conducive to the extension of the primer, so that when the temperature rises to 42 °C, the primer is still in hybridization state. The sample is heated at 95 °C for 5 min and then placed at 0–5 °C for 5 min. Finally, CT values were obtained and calculated by the 2^{-ΔΔct} method. GAPDH and U6 was selected as the housekeeping gene. The primer sequences were as follows (5' → 3'):

In addition, for RNaseR digestion, RNA was mixed with RNaseR enzyme in a reaction buffer following the manufacturer's instructions. Importantly, a control sample without RNaseR (Mock group) was also prepared to compare the degradation efficiency and validate experimental outcomes. The mixture was incubated at 37 °C for 30 min. Then the levels of circ-PSMB1 and line-PSMB1 were detected by qRT-PCR.

circ-PSMB1, Forward Primer CAGCAAGTGCCATGCTACAG, Reverse Primer CCGCGTATGAATTGAAAAC C.

miR-624-3p, Forward Primer GCCGAGCACAAGGU AUUGGU, Reverse Primer CTCAACTGGTGTCTGG A.

IL-1β, Forward Primer CTGTGTCTTTCCCGTGGAC C, Reverse Primer CAGCTCATATGGGTCCGACA.

IL-18, Forward Primer ATCGCTTCCTCTCGCAACA A, Reverse Primer GTCCGGGGTGCATTATCTCT.

ASC, Forward Primer GTTCCTCCGGGACTATGAT GC, Reverse Primer GCGTCTCGTCCAAGACTGATG.

GAPDH, Forward Primer GGAGCGAGATCCCTCCA AAAT, Reverse Primer GGCTGTTGTCATACTTCTCA TGG.

U6, Forward Primer GCTTCGGCAGCACATATACT AAAAT, Reverse Primer CGCTTCACGAATTTGCGTG TCAT.

MTT assay

Cell viability was determined by MTT assay. HAECs were seeded in 96-well plates and cultured for 48 h. Then, the cells were incubated with 5 mg/mL MTT solution for 4 h. Next, the culture medium was discarded, and 150 µL of DMSO solution was added to each well. The plate was shaken slightly with a thermostatic vibrator for 10 min. Finally, the absorbance value (OD value) of each well was measured at 490 nm with a microplate reader.

Flow cytometry

The cell pyroptosis was detected according to a previous study [28]. The Active caspase-1 Pyroptosis Detection

Kit purchased from Sungene Biotech (Tianjin, China) was employed for Active caspase-1/propidium iodide (PI) double-staining. Briefly, HAECs were digested and washed with PBS 2 times. Next, the cells were centrifuged (3000 r, 5 min), and the precipitate was resuspended in binding buffer at a density of 1×10^6 cell/mL. Then, the cells were mixed with 5 μ l of active caspase-1 and 5 μ l of PI and incubated in the dark at room temperature for 15 min. Finally, the pyroptotic cells were analysed by flow cytometry (BD Biosciences, San Jose, CA, USA). The PI-positive cells represented pyroptotic cells.

Determination of LDH levels

HAECs were centrifuged at 400 \times g for 5 min to get supernatant. Then, the LDH levels of the supernatant were determined with a kit provided by Beyotime Biotechnology Co., Ltd. (C0016, Jiangsu, China). All the operations were carried out in strict accordance with the kit instructions.

Western blotting

Anti-NLRP3 (ab263899, 1:1000) and anti-GSDMD-N (ab215203, 1:800) antibodies were obtained from Abcam (CA, USA). RIPA lysis buffer (Beyotime) was used to isolate the proteins from the cells. Next, 40 μ g of protein was separated by twelve alkyl sulfate polyacrylamide gel electrophoresis and transferred to PVDF membranes. Then, the membranes were removed, and 5% skim milk was used to block the membranes for 1 h. After washing 3 times, the membranes were incubated with the primary antibodies for 12 h at 4 °C. Then, the membranes were washed and incubated with the secondary antibody (ab288151, Abcam). Finally, the membranes were analysed with an ECL Kit (Beyotime), and the grey value was calculated by ImageJ software.

Dual-luciferase reporter assay

Psi-circ-PSMB1/ASC-3'-UTR wild type (WT) and Psi-circ-PSMB1/ASC-3'-UTR mutant type (MUT) reporter plasmids were synthesized in advance. According to the instructions, HAECs were cotransfected with miR-624-3p mimics or miR-624-3p inhibitor together with 0.1 μ g psi-circ-PSMB1/ASC-3'-UTR WT or psi-circ-PSMB1/ASC-3'-UTR MUT reporter plasmids using Lipofectamine 2000. After 48 h, the Dual-luciferase Reporter Assay System (Promega, USA) was used to measure the luciferase activities.

RNA pull-down assay

HAECs were transfected with 50 nM of biotinylated miR-624-3p probe (3'-end biotinylated, synthesized by GenePharma Co., Ltd.) or equivalent amount of biotinylated scramble negative control probe (NC probe, 5'-CAG UACUUUUGUGUAGUACAA-3') using Lipofectamine

3000 reagent. After 48 h of transfection, cells were collected and washed twice with cold PBS. The cell pellets were lysed in NP-40 lysis buffer supplemented with RNase inhibitor and protease inhibitor cocktail for 10 min on ice. The lysates were then incubated with pre-washed M-280 streptavidin magnetic beads (Thermo Fisher Scientific) at 4 °C for 3 h with gentle rotation. Following three washes with high-salt buffer (500 mM NaCl, 10 mM Tris-HCl, pH 7.5), the bead-bound RNA complexes were eluted and purified using TRIzol LS reagent. The enrichment of circ-PSMB1 and ASC was subsequently quantified by RT-qPCR with specific primers spanning the circular junction or linear transcript regions, respectively.

Statistical analysis

All the experiments were repeated at least 3 times. The data were analysed by using SPSS 21.0 and are presented as the mean \pm standard deviation. The results were evaluated using the T test for the comparison of two samples and one-way ANOVA for the comparison of more than two samples. Differences between groups were considered significant when $p < 0.05$.

Results

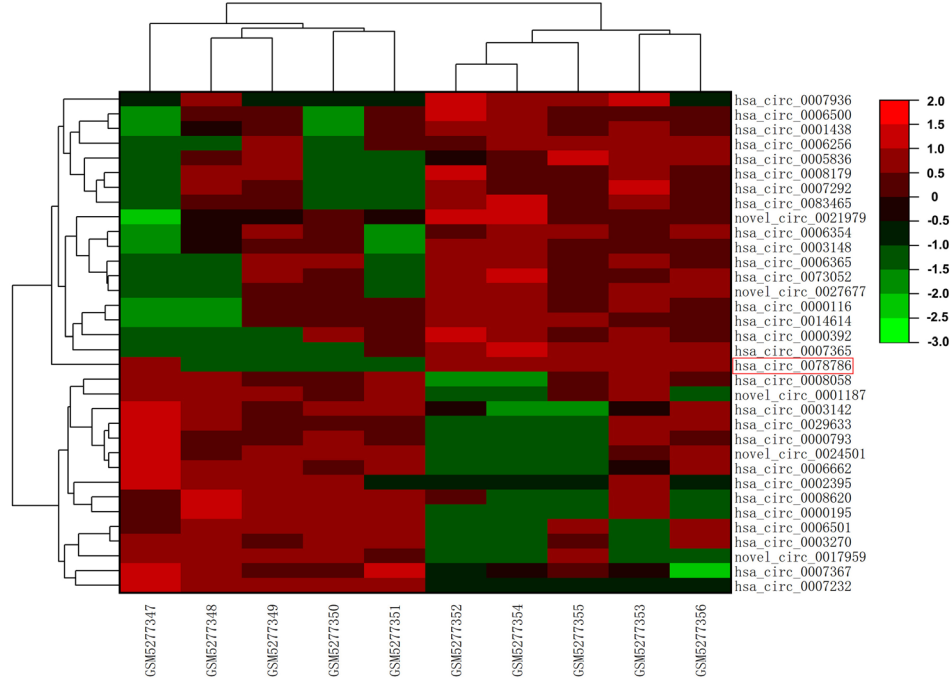
Circ-PSMB1 was elevated in ox-LDL-stimulated HAECs

According to the results shown in the heatmap and volcano maps, hsa_circ_0007232 was the most significantly downregulated circular RNA, while hsa_circ_0078786 (circ-PSMB1) was the most significantly up-regulated circular RNA. For the clinical significance analysis of molecular markers, high expression genes are usually selected instead of low expression ones. Therefore, circ-PSMB1 was selected for next experiments (Fig. 1A and B). In addition, we also found that circ_0078786 was substantially elevated in serum samples of AS patients (Fig. 1C). From CircPrimer software, we found that circ_0078786 is formed by splicing exons 2 and 3 on chromosome 6. PSMB1 was the parental gene (Fig. 1D). Then, RnaseR was used to analyze the RNA stability. We found that RnaseR significantly decreased the levels line-PSMB1 and showed no effects on circ-PSMB1 (Fig. 1E). Next, we establish the AS cell model using HAECs and smooth muscle cells. We found that circ-PSMB1 was increased in ox-LDL-stimulated HAECs, and showed no change in ox-LDL-stimulated smooth muscle cells (Fig. 1F and G). Therefore, ox-LDL-stimulated HAECs was used for next experiments. The FISH assay showed that circ_0078786 was mainly located in the cytoplasm of HAECs (Fig. 1H).

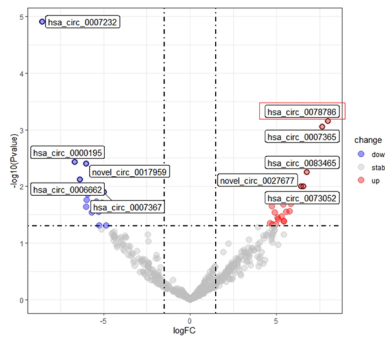
Downregulation of circ-PSMB1 decreased the pyroptosis rate of ox-LDL-treated HAECs

HAECs were transfected with si-circ-PSMB1 #1 and #2, both of which strongly decreased circ-PSMB1 expression,

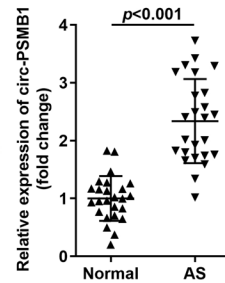
A



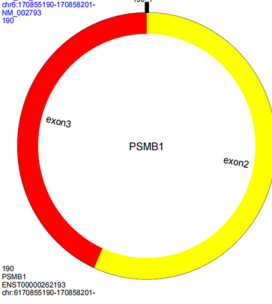
B



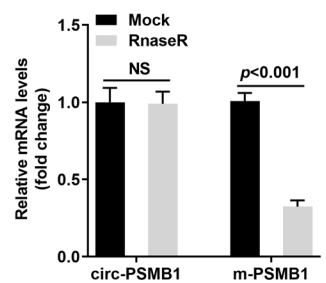
C



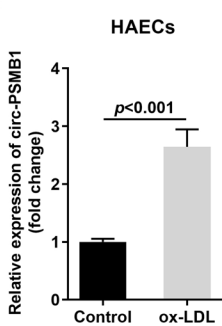
D



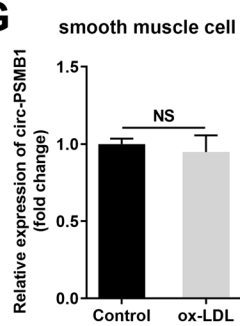
E



F



G



H

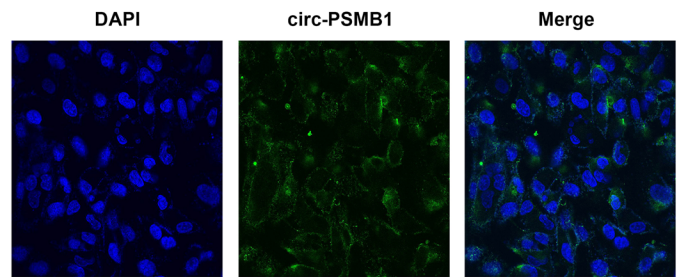


Fig. 1 Circ-PSMB1 was elevated in ox-LDL-stimulated HAECs. Heatmap (A) and volcano map (B) of the differentially expressed circRNAs in AS. (C) The circ-PSMB1 levels in the serum of AS patients were analyzed by qRT-PCR. (D) The structure of circ-PSMB1. (E) The circ-PSMB1 and line-PSMB1 levels in HAECs were detected by qRT-PCR after RnaseR treatment. The circ-PSMB1 level in ox-LDL treated HAECs (F) and smooth muscle cells (G) were detected by RT-qPCR. (H) The location of circ-PSMB1 was tested by FISH assay

and si-circ-PSMB1 #1 exerted a better effect. We selected si-circ-PSMB1 #1 for use in the next experiments (Fig. 2A). Next, after ox-LDL stimulation, the viability of the HAECs was substantially decreased. Si-circ-PSMB1 substantially enhanced the viability of ox-LDL-treated HAECs (Fig. 2B). In addition, ox-LDL stimulation strongly enhanced the pyroptosis rate of HAECs, and

si-circ-PSMB1 substantially decreased the pyroptosis rate of ox-LDL-treated HAECs (Fig. 2C). Additionally, the LDH level (Fig. 2D), the IL-1 β (Fig. 2E) and IL-18 (Fig. 2F) mRNA levels, and the NLRP3 and GSDMD-N protein levels (Fig. 2G) were substantially enhanced after ox-LDL stimulation. Si-circ-PSMB1 transfection greater decreased the levels of these factors.

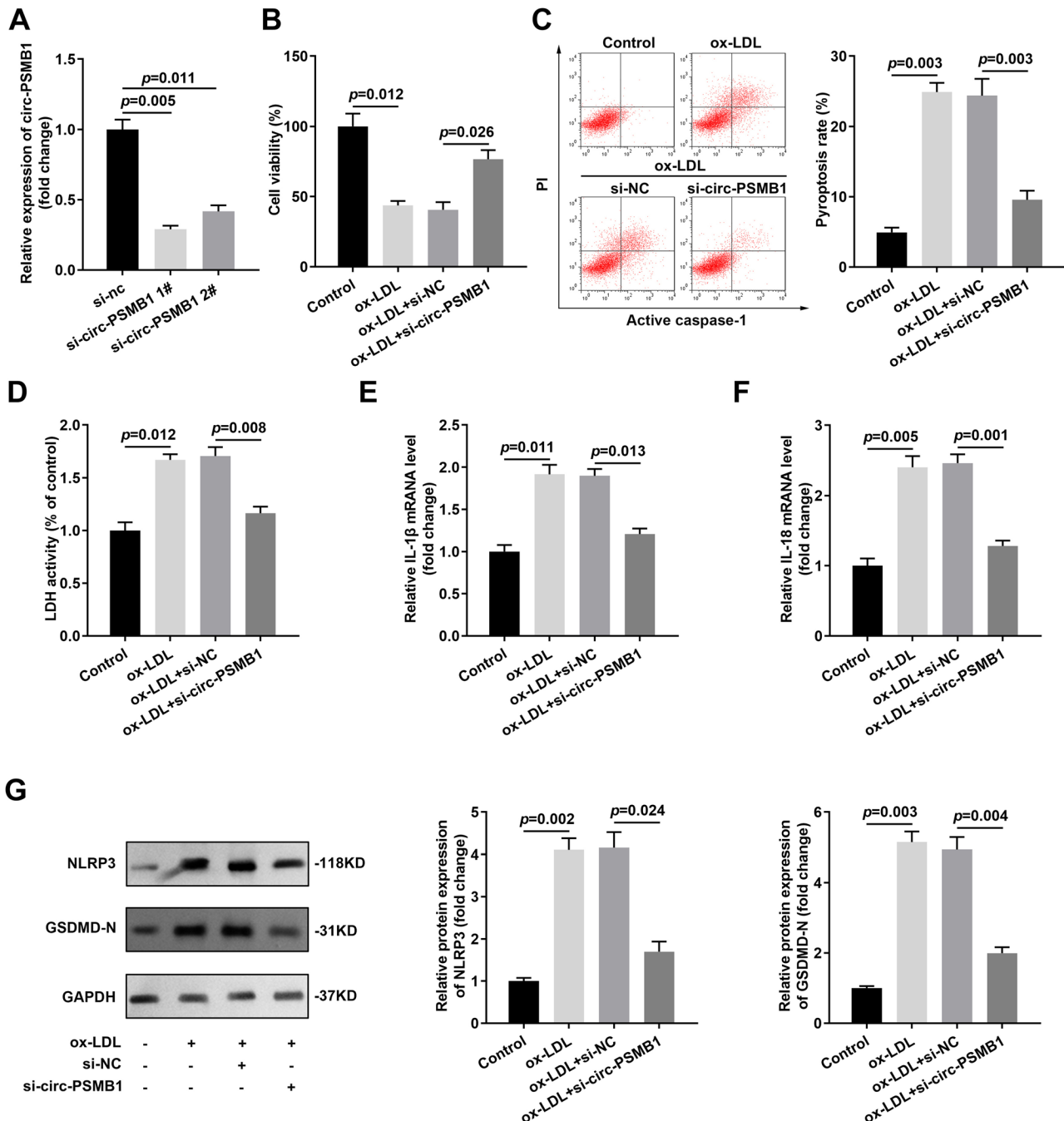


Fig. 2 Downregulation of circ-PSMB1 decreased the pyroptosis of ox-LDL-treated HAECs. (A) The circ-PSMB1 levels were analysed by qRT-PCR after si-circ-PSMB1 #1 and #2 transfection. After si-circ-PSMB1 transfection, (B) cell viability was measured by MTT assay, (C) the pyroptosis rate was analysed by flow cytometry, (D) LDH levels were measured with the corresponding kit, (E-F) IL-1 β and IL-18 levels were determined by qRT-PCR, and (G) the protein expression levels of NLRP3 and GSDMD-N were analysed by western blotting

Circ-PSMB1 sponged miR-624-3p in HAECs

With starBase software, we selected we found that miR-624-3p was a direct target of circ-PSMB1 (Fig. 3A). In addition, WT circ-PSMB1 strongly decreased the luciferase activity of miR-624-3p but not MUT circ-PSMB1 (Fig. 3B). In addition, biotin-miR-624-3p greatly enhanced the enrichment of circ-PSMB1 compared with biotin-NC (Fig. 3C). Moreover, the miR-624-3p levels were strongly depleted in ox-LDL-treated HAECs (Fig. 3D), and si-circ-PSMB1 substantially enhanced the miR-624-3p levels in ox-LDL treated HAECs (Fig. 3E).

Downregulation of miR-624-3p neutralized the effects of si-circ-PSMB1 in ox-LDL-treated HAECs

The miR-624-3p levels were greatly decreased after miR-624-3p inhibitor transfection and enhanced after miR-624-3p mimic transfection (Fig. 4A). Additionally, the miR-624-3p inhibitor substantially neutralized the effects of si-circ-PSMB1 on cell viability (Fig. 4B), pyroptosis (Fig. 4C), LDH levels (Fig. 4D), IL-1 β (Fig. 4E) and IL-18 (Fig. 4F) mRNA levels, and NLRP3 and GSDMD-N protein levels (Fig. 4G). Furthermore, we also explored the role of miR-624-3p mimic in ox-LDL treated HAECs. MiR-624-3p overexpression promoted the cell viability, inhibited pyroptosis, LDH levels, IL-1 β and IL-18 mRNA

levels, and NLRP3 and GSDMD-N protein levels in ox-LDL treated HAECs (Supplementary Fig. 1). In addition, we used an oligonucleotide target-site blocker (TSB) to prevents circPMBP1-miR-624 binding. The results showed that TSB treatment promoted the cell viability, inhibited pyroptosis, LDH levels, IL-1 β and IL-18 mRNA levels, and NLRP3 and GSDMD-N protein levels in ox-LDL treated HAECs (Supplementary Fig. 2).

miR-624-3p targeted ASC in HAECs

With TargetScan software, we obtained 3711 target genes of miR-624-3p. Among them, ASC was a key gene involved in pyroptosis. So. We selected ASC as a direct target gene of miR-624-3p for next experiments (Fig. 5A). In addition, WT ASC strongly decreased the luciferase activity of miR-624-3p but not that of MUTASC (Fig. 5B). In addition, biotin-miR-624-3p greatly enhanced the enrichment of ASC compared with biotin-NC (Fig. 5C). Moreover, the ASC levels were substantially enhanced in ox-LDL-treated HAECs (Fig. 5D), and the miR-624-3p mimic greatly decreased the ASC levels (Fig. 5E). In addition, circ-PSMB1 knockdown significantly decreased ASC levels in the ox-LDL-treated HAECs (Fig. 5F).

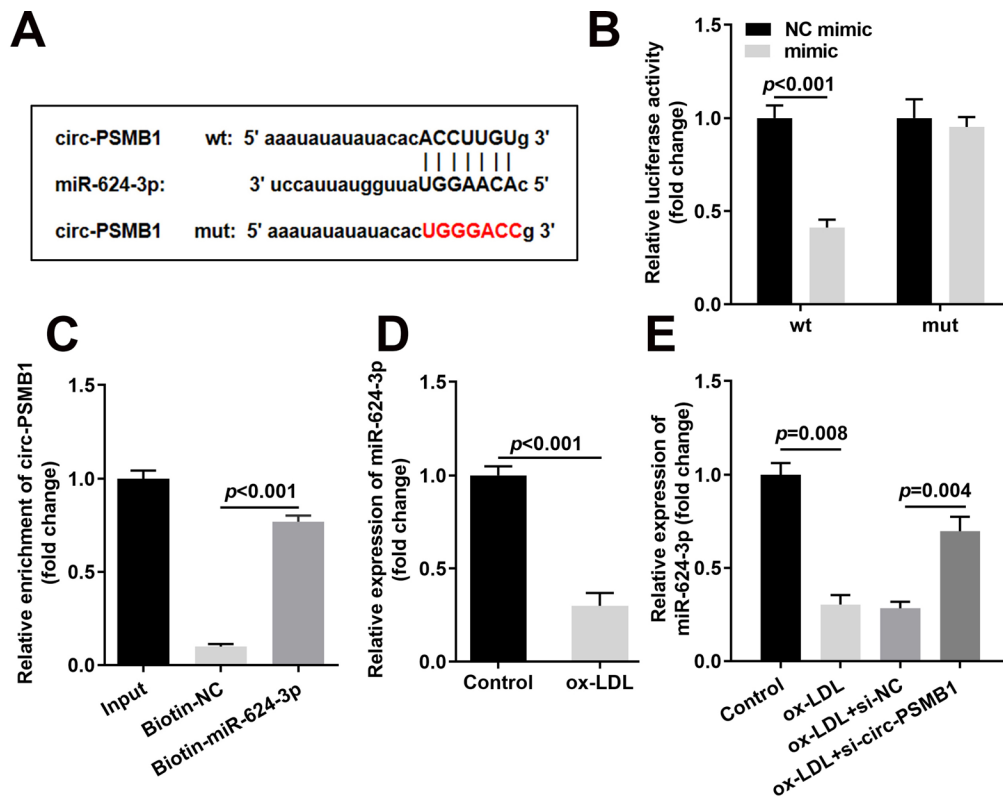


Fig. 3 Circ-PSMB1 sponged miR-624-3p in HAECs. (A) Binding sites between circ-PSMB1 and miR-624-3p. The relationship between circ-PSMB1 and miR-624-3p was examined by dual-luciferase reporter (B) and RNA pull-down (C) assays. The miR-624-3p levels were measured by qRT-PCR after ox-LDL (D) and si-circ-PSMB1 (E) treatment

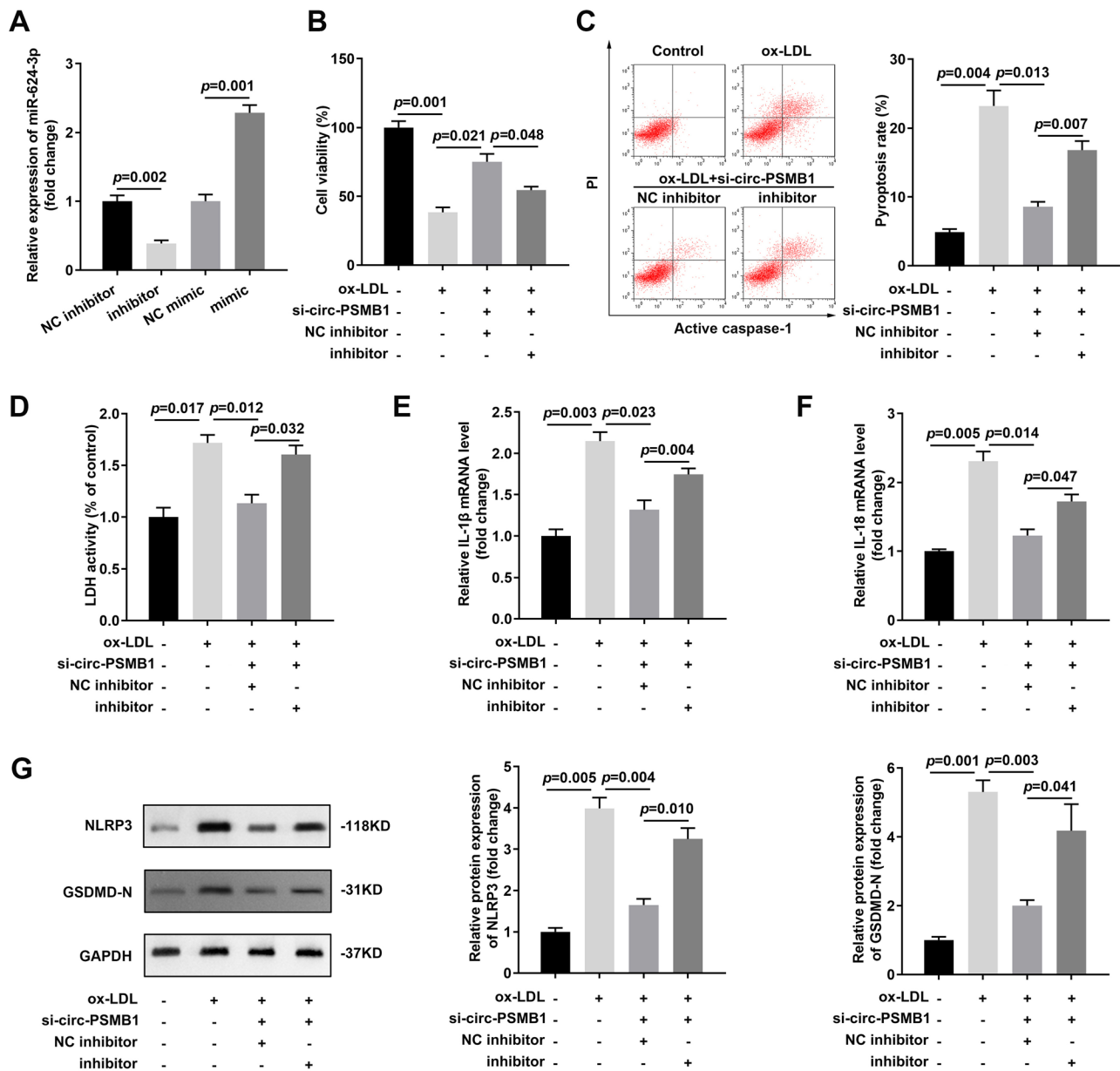


Fig. 4 Downregulation of miR-624-3p neutralized the effects of si-circ-PSMB1 in ox-LDL-treated HAECs. **(A)** The miR-624-3p levels were measured by qRT-PCR after miR-624-3p mimic and inhibitor treatment. After si-circ-PSMB1 and miR-624-3p inhibitor transfection, **(B)** cell viability was measured by MTT assay, **(C)** the pyroptosis rate was analysed by flow cytometry, **(D)** LDH levels were measured with the corresponding kit, **(E-F)** IL-1 β and IL-18 levels were determined by qRT-PCR, and **(G)** the protein expression levels of NLRP3 and GSDMD-N were analysed by western blotting

Upregulation of ASC neutralized the effects of miR-624-3p in ox-LDL-treated HAECs

The ASC levels were greatly enhanced after ASC vector transfection (Fig. 6A). Next, we found that the miR-624-3p mimic substantially enhanced the viability of ox-LDL-stimulated HAECs, while overexpressing ASC greatly decreased the viability (Fig. 6B). Additionally, the miR-624-3p mimic substantially decreased the pyroptosis rate (Fig. 6C), LDH levels (Fig. 6D), IL-1 β (Fig. 6E) and IL-18 (Fig. 6F) mRNA levels, and NLRP3 and GSDMD-N protein levels (Fig. 6G) in ox-LDL-treated HAECs,

while upregulation of ASC neutralized the effects of miR-624-3p. Furthermore, we also explored the role of ASC knockdown in ox-LDL treated HAECs. ASC knockdown promoted the cell viability, inhibited pyroptosis, LDH levels, IL-1 β and IL-18 mRNA levels, and NLRP3 and GSDMD-N protein levels in ox-LDL treated HAECs (Supplementary Fig. 3).

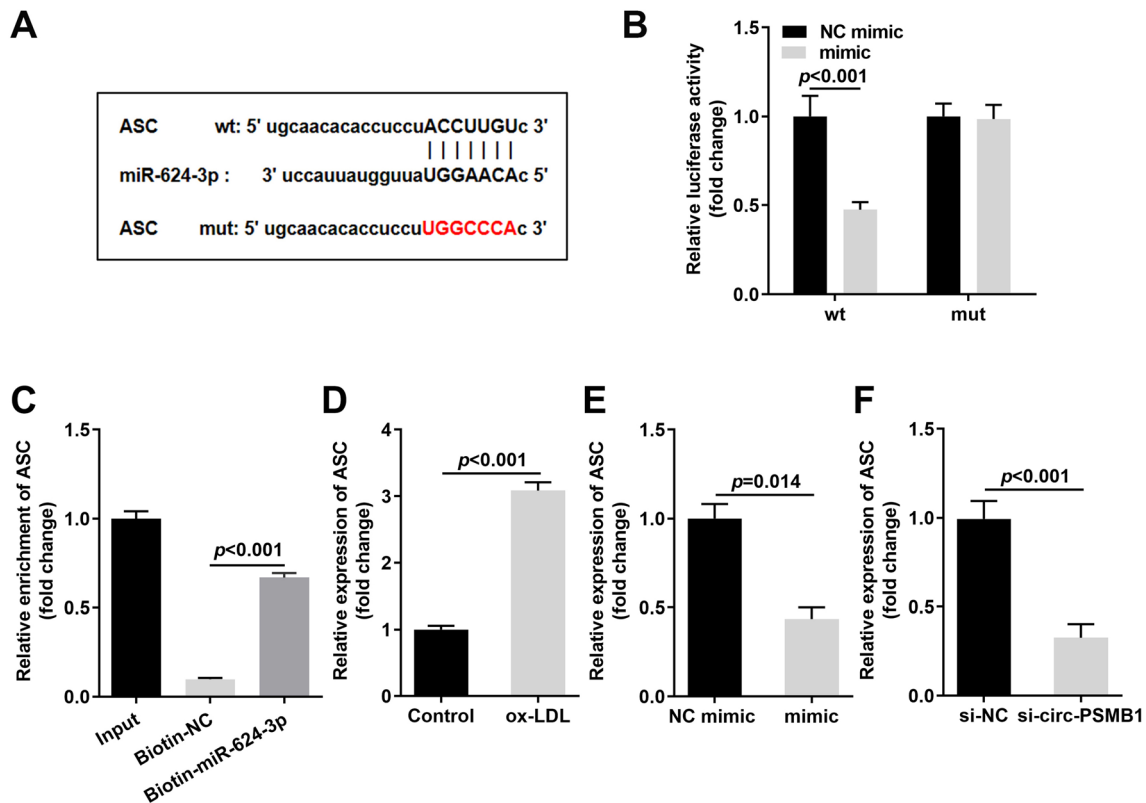


Fig. 5 miR-624-3p targeted ASC in HAECs. **(A)** Binding sites between miR-624-3p and ASC. The relationship between miR-624-3p and ASC was examined by dual-luciferase reporter **(B)** and RNA pull-down **(C)** assays. The ASC levels were measured by qRT-PCR after ox-LDL **(D)** as well as miR-624-3p mimic **(E)** treatment. **(F)** The ASC levels in ox-LDL treated HAECs were measured by qRT-PCR after circ-PSMB1 knockdown

Discussion

Here, we demonstrated that circ-PSMB1 was overexpressed in ox-LDL-treated HAECs. In addition, circ-PSMB1 silencing mitigated pyroptosis in ox-LDL-treated HAECs by modulating the miR-624-3p/ASC axis.

Recently, circRNAs were demonstrated to be involved in the pathological development of many diseases, and their potential mechanism may be closely related to the upregulation or downregulation of circRNA expression [29, 30]. Lin et al. [31] showed that 73 circRNAs were upregulated and 37 circRNAs were downregulated in the peripheral blood of patients with coronary heart disease characterized by AS. Wei et al. [32] confirmed that circHIPK3 suppressed the lipid content in HUVECs treated with ox-LDL by modulating cell autophagy. In addition, Ding et al. [33] demonstrated that circ_0010283 was overexpressed in VSMCs treated with ox-LDL, and circ_0010283 silencing inhibited the growth of VSMCs. These studies demonstrated that circRNAs are of great significance to the occurrence and development of AS. Similarly, in this research, through bioinformatic analysis, we found that circ-PSMB1 was overexpressed in AS, which was further demonstrated in ox-LDL-treated HAECs.

In recent years, substantial evidence has shown that cell death occurs in all major cell types in AS lesions [34, 35]. Pyroptosis is a newly discovered and confirmed mode of programmed cell death. The occurrence of pyroptosis depends on the upstream inflammasomes and caspase-1. Among related molecules, NLRP3 inflammasomes are the most widely studied [36]. Previous research showed that compared with control samples, NLRP3 was highly expressed in the aortas of patients with coronary AS and was positively correlated with the severity of coronary artery disease, confirming that NLRP3 was also a risk factor for AS [37]. In addition, studies have shown that GSDMD is involved in pyroptosis. The formation of pores by its N-terminal fragment is the driving factor of pyroptosis [38, 39]. In this study, we found that ox-LDL induced pyroptosis in HAECs, as shown by the increased protein expression of NLRP3 and GSDMD-N. In addition, the upregulation of the mRNA expression of IL-1 β indicated that the inflammatory reaction also occurred in ox-LDL-treated HAECs. Interestingly, after circ-PSMB1 silencing, pyroptosis in ox-LDL-treated HAECs was inhibited. These results implied that circ-PSMB1 might promote AS progression by inducing pyroptosis in endothelial cells. However, the mechanism by which

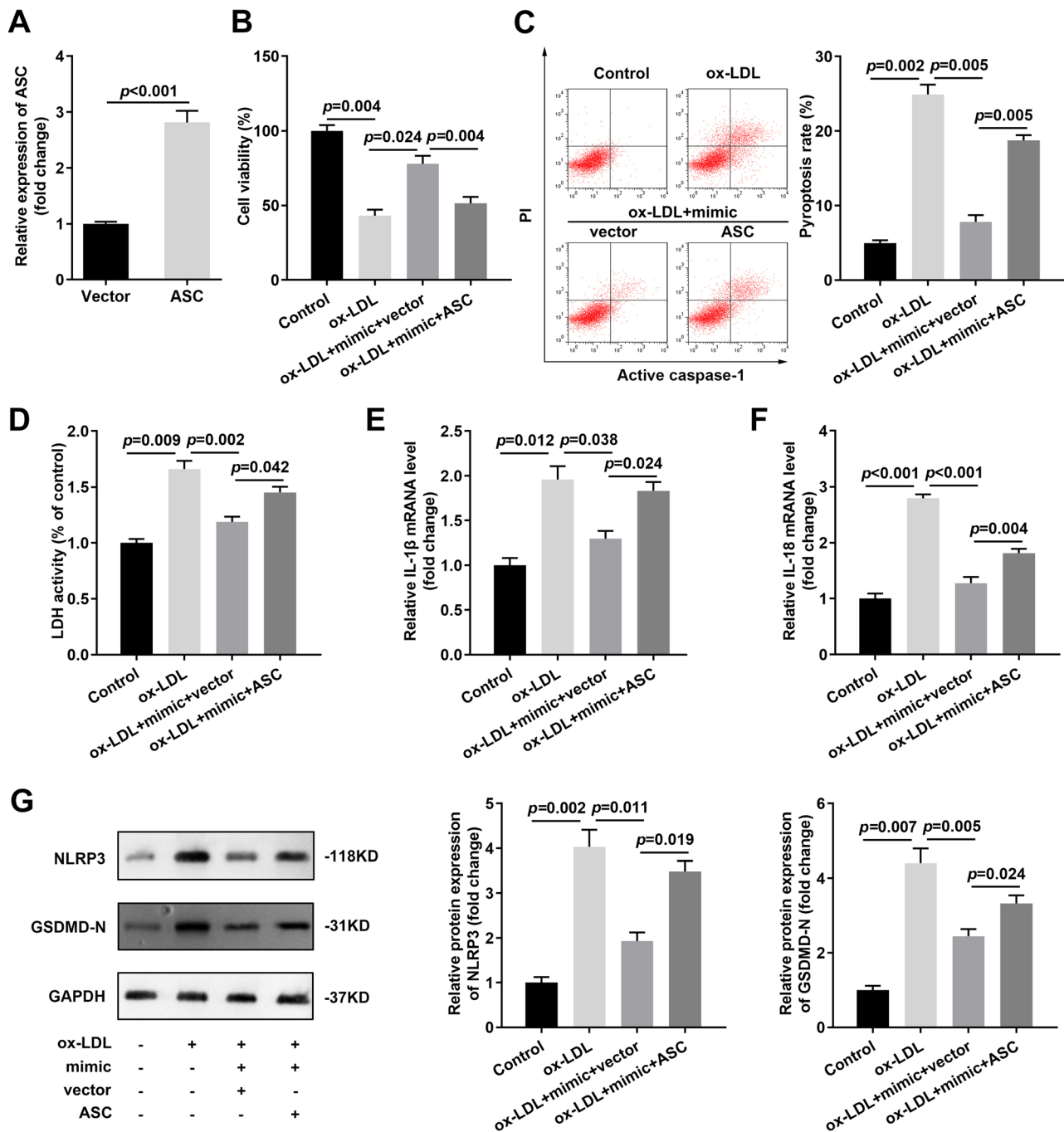


Fig. 6 Upregulation of ASC neutralized the effects of miR-624-3p in ox-LDL-treated HAECs. **(A)** The ASC levels were measured by qRT-PCR after ASC vector treatment. After miR-624-3p mimic and ASC transfection, **(B)** cell viability was measured by MTT assay, **(C)** the pyroptosis rate was analysed by flow cytometry, **(D)** LDH levels were measured with the corresponding kit, **(E-F)** IL-1 β and IL-18 levels were determined by qRT-PCR, and **(G)** the protein expression levels of NLRP3 and GSDMD-N were analysed by western blotting

circ-PSMB1 increased the level of NLRP3 is unclear and requires further research.

To understand the specific mechanism by which circ-PSMB1 functions in AS, we screened the miRNAs that target circ-PSMB1 and confirmed that miR-624-3p targets circ-PSMB1. miRNAs are endogenous noncoding RNAs with a length of 21 ~ 25 nt that are widely expressed

in eukaryotes and are important noncoding RNAs that regulate protein biosynthesis [40]. Recently, various studies have revealed that miRNAs play a vital role in AS progression. For example, Zhu et al. [41] found that miR-21-3p accelerates AS progression by increasing vascular smooth muscle cell growth. Guo et al. [42] demonstrated that miR-23a-3p modulates inflammation as well as cell

apoptosis in AS via the NF- κ B and p38/MAPK signalling pathways. However, whether miR-624-3p is involved in the regulation of AS has not been reported. In this study, we confirmed that miR-624-3p was decreased in ox-LDL-treated HAECs. Downregulation of miR-624-3p neutralized the effects of si-circ-PSMB1 on the cell pyroptosis of ox-LDL-treated HAECs. Subsequently, through bioinformatics analysis, we confirmed that ASC was the target gene of miR-624-3p. Recently, various circRNAs have been proven to function as ceRNAs to inhibit the binding of miRNA to mRNAs in AS [33, 43, 44]. In this study, we found that overexpressing ASC neutralized the effects of miR-624-3p on the pyroptosis of ox-LDL-treated HAECs, which indicated that circ-PSMB1 participated in AS progression by modulating the miR-624-3p/ASC axis. Previous research confirmed that in response to endogenous and exogenous stimulation, ASC acts on pro-caspase-1 to form inflammasomes and activate pro-caspase-1. Activated caspase-1 induces the activation of downstream cytokines, including IL-1 β and IL-18. This leads to the secretion of LDH, which eventually results in cell injury and pyroptosis [45]. Therefore, these findings further illustrated that circ-PSMB1 participated in AS progression by modulating the pyroptosis of endothelial cells.

In summary, this research demonstrated that circ-PSMB1 and ASC were overexpressed and that miR-624-3p was expressed at low levels in ox-LDL-treated HAECs. circ-PSMB1 might participated in AS progression by modulating the miR-624-3p/ASC axis. This study reported the mechanism of circ-PSMB1 in AS for the first time, and explored the regulation of circ-PSMB1 in the development of AS by establishing a cell model and using pyroptosis detection technology. Our research provided scientific guidance and suggestions for the precise treatment of AS and the development of targeted drugs in future. However, there are still some limitation in this study. Due to limitations in experimental conditions, we did not conduct animal experiments for verification. However, our future research will conduct in-depth research on the role of circ-PSMB1 in animal models to improve the mechanism of circ-PSMB1 in AS.

Supplementary Information

The online version contains supplementary material available at <https://doi.org/10.1186/s13019-025-03457-z>.

Supplementary Material 1

Acknowledgements

Not applicable.

Author contributions

All authors participated in the design, interpretation of the studies and analysis of the data and review of the manuscript. Y Z drafted the work and revised it critically for important intellectual content; Y G was responsible for the acquisition, analysis and interpretation of data and provided the

conception and design of the work. All authors read and approved the final manuscript.

Funding

The work was supported by Key Clinical Subject Construction Program of Chongqing.

Data availability

The datasets used and/or analysed during the current study are available from the corresponding author on reasonable request.

Declarations

Ethics approval and consent to participate

This study was approved by the Ethics Committee of Jiangjin Centre Hospital. Informed consent was obtained from all individual participants included in the study. This study was performed in line with the principles of the Declaration of Helsinki. All methods were carried out in accordance with relevant guidelines and regulations.

Consent for publication

Not applicable.

Competing interests

The authors declare no competing interests.

Received: 17 December 2024 / Accepted: 21 April 2025

Published online: 02 May 2025

References

- Zhu Y, Xian X, Wang Z, Bi Y, Chen Q, Han X, Tang D, Chen R. Research progress on the relationship between atherosclerosis and inflammation. *Biomolecules* (Basel Switzerland). 2018;8(3):80.
- Latic N, Erben RG. Vitamin D and Cardiovascular Disease, with Emphasis on Hypertension, Atherosclerosis, and Heart Failure. *INT J MOL SCI* 2020, 21(18).
- Lee YJ, Han BH, Yoon JJ, Kim HY, Ahn YM, Hong MH, Son CO, Kang DG, Lee HS. Identification of securinine as vascular protective agent targeting atherosclerosis in vascular endothelial cells, smooth muscle cells, and Apolipoprotein E deficient mice. *Phytomedicine*. 2021;81:153430.
- Kim SM, Huh JW, Kim EY, Shin MK, Park JE, Kim SW, Lee W, Choi B, Chang EJ. Endothelial dysfunction induces atherosclerosis: increased Aggrecan expression promotes apoptosis in vascular smooth muscle cells. *BMB REP*. 2019;52(2):145–50.
- Libby P. The changing landscape of atherosclerosis. *Nature*. 2021;592(7855):524–33.
- Björkegren JLM, Lusis AJ. Atherosclerosis: Recent developments. *CELL* 2022, 185(10):1630–1645.
- Peter Libby JE, Buring L, Badimon GöranK, Hansson. John Deanfield, Márcio Sommer Bittencourt, Lale Tokgözoğlu, Lewis EF: atherosclerosis. *NAT REV DIS PRIMERS* 2019, (1)(5):56.
- Gupta M, Blumenthal C, Chatterjee S, Bandyopadhyay D, Jain V, Lavie CJ, Virani SS, Ray KK, Aronow WS, Ghosh RK. Novel emerging therapies in atherosclerosis targeting lipid metabolism. *EXPERT OPIN INV DRUG*. 2020;29(6):611–22.
- Di Pietro N, Formoso G, Pandolfi A. Physiology and pathophysiology of OxLDL uptake by vascular wall cells in atherosclerosis. *VASC PHARMACOL*. 2016;84:1–7.
- Kattoor AJ, Kanuri SH, Mehta JL. Role of Ox-LDL and LOX-1 in atherogenesis. *CURR MED CHEM*. 2019;26(9):1693–700.
- Li Y, Niu X, Xu H, Li Q, Meng L, He M, Zhang J, Zhang Z, Zhang Z. VX-765 attenuates atherosclerosis in ApoE deficient mice by modulating VSMCs pyroptosis. *EXP CELL RES*. 2020;389(1):111847.
- Meng Q, Li Y, Ji T, Chao Y, Li J, Fu Y, Wang S, Chen Q, Chen W, Huang F, et al. Estrogen prevent atherosclerosis by attenuating endothelial cell pyroptosis via activation of Estrogen receptor alpha-mediated autophagy. *J ADV RES*. 2021;28:149–64.
- Shi J, Gao W, Shao F. Pyroptosis: Gasdermin-Mediated programmed necrotic cell death. *TRENDS BIOCHEM SCI*. 2017;42(4):245–54.

14. Gu L, Sun M, Li R, Zhang X, Tao Y, Yuan Y, Luo X, Xie Z. Didymin suppresses microglia pyroptosis and neuroinflammation through the Asc/Caspase-1/GSDMD pathway following experimental intracerebral hemorrhage. *FRONT IMMUNOL*. 2022;13:810582.
15. Gan Z, Guo Y, Zhao M, Ye Y, Liao Y, Liu B, Yin J, Zhou X, Yan Y, Yin Y, et al. Excitatory amino acid transporter supports inflammatory macrophage responses. *Sci Bull (Beijing)*. 2024;69(15):2405–19.
16. Zhou W, Cai Z, Liu J, Wang D, Ju H, Xu R. Circular RNA: metabolism, functions and interactions with proteins. *MOL CANCER*. 2020;19(1):172.
17. Kristensen LS, Andersen MS, Stagsted LW, Ebbesen KK, Hansen TB, Kjems J. The biogenesis, biology and characterization of circular RNAs. *Nat Rev Genet*. 2019;20(11):675–91.
18. Li X, Yang L, Chen L. The biogenesis, functions, and challenges of circular RNAs. *MOL CELL*. 2018;71(3):428–42.
19. Xiao W, Li J, Hu J, Wang L, Huang JR, Sethi G, Ma Z. Circular RNAs in cell cycle regulation: mechanisms to clinical significance. *CELL PROLIFERAT*. 2021;54(12):e13143.
20. Cheng Y, Su Y, Wang S, Liu Y, Jin L, Wan Q, Liu Y, Li C, Sang X, Yang L et al. Identification of circRNA-lncRNA-miRNA-mRNA Competitive Endogenous RNA Network as Novel Prognostic Markers for Acute Myeloid Leukemia. *GENES-BASEL* 2020, 11(8).
21. Zheng Q, Bao C, Guo W, Li S, Chen J, Chen B, Luo Y, Lyu D, Li Y, Shi G, et al. Circular RNA profiling reveals an abundant circHIPK3 that regulates cell growth by sponging multiple miRNAs. *NAT COMMUN*. 2016;7(1):11215.
22. Shen L, Hu Y, Lou J, Yin S, Wang W, Wang Y, Xia Y, Wu W. CircRNA0044073 is upregulated in atherosclerosis and increases the proliferation and invasion of cells by targeting miR107. *MOL MED REP*. 2019;19(5):3923–32.
23. Tong K, Tan K, Lim Y, Tien X, Wong P. CircRNA-miRNA interactions in atherosclerosis. *MOL CELL BIOCHEM*. 2022;477(12):2703–33.
24. Farina FM, Weber C, Santovito D. The emerging landscape of non-conventional RNA functions in atherosclerosis. *ATHEROSCLEROSIS*. 2023;374:74–86.
25. Yang J, Rong S. The emerging role of circRNAs in atherosclerosis. *CURR VASC PHARMACOL*. 2023;21(1):26.
26. Paone S, Baxter AA, Hulett MD, Poon I. Endothelial cell apoptosis and the role of endothelial cell-derived extracellular vesicles in the progression of atherosclerosis. *CELL MOL LIFE SCI*. 2019;76(6):1093–106.
27. Xing X, Li Z, Yang X, Li M, Liu C, Pang Y, Zhang L, Li X, Liu G, Xiao Y. Adipose-derived mesenchymal stem cells-derived exosome-mediated microRNA-342-5p protects endothelial cells against atherosclerosis. *Aging*. 2020;12(4):3880–98.
28. Li MY, Zhu XL, Zhao BX, Shi L, Wang W, Hu W, Qin SL, Chen BH, Zhou PH, Qiu B, et al. Adrenomedullin alleviates the pyroptosis of Leydig cells by promoting autophagy via the ROS-AMPK-mTOR axis. *CELL DEATH DIS*. 2019;10(7):489.
29. Li X, Ding J, Wang X, Cheng Z, Zhu Q. NUDT21 regulates circRNA cyclization and CeRNA crosstalk in hepatocellular carcinoma. *Oncogene*. 2020;39(4):891–904.
30. Yu L, Liu Y. circRNA_0016624 could sponge miR-98 to regulate BMP2 expression in postmenopausal osteoporosis. *BIOCHEM BIOPH RES CO*. 2019;516(2):546–50.
31. Lin F, Zhao G, Chen Z, Wang X, Lv F, Zhang Y, Yang X, Liang W, Cai R, Li J, et al. circRNA-miRNA association for coronary heart disease. *MOL MED REP*. 2019;19(4):2527–36.
32. Wei MY, Lv RR, Teng Z. Circular RNA circHIPK3 as a novel circRNA regulator of autophagy and endothelial cell dysfunction in atherosclerosis. *EUR REV MED PHARMACO*. 2020;24(24):12849–58.
33. Ding P, Ding Y, Tian Y, Lei X. Circular RNA circ_0010283 regulates the viability and migration of oxidized lowdensity lipoprotein-induced vascular smooth muscle cells via an miR3703p/HMGB1 axis in atherosclerosis. *INT J MOL MED*. 2020;46(4):1399–408.
34. Li M, Wang Z, Fang L, Cheng S, Wang X, Liu N. Programmed cell death in atherosclerosis and vascular calcification. *CELL DEATH DIS*. 2022;13(5):467.
35. Grootaert MOJ, Moulis M, Roth L, Martinet W, Vindis C, Bennett MR, De Meyer GRY. Vascular smooth muscle cell death, autophagy and senescence in atherosclerosis. *CARDIOVASC RES*. 2018;114(4):622–34.
36. Coll RC, Schroder K, Pelegrin P. NLRP3 and pyroptosis blockers for treating inflammatory diseases. *TRENDS PHARMACOL SCI*. 2022;43(8):653–68.
37. Zheng FM, Xing SP, Gong ZM, Xing QM. NLRP3 inflammasomes show high expression in aorta of patients with atherosclerosis. *Heart Lung Circ*. 2013;22(9):746–50.
38. Zuo Y, Chen L, Gu H, He X, Ye Z, Wang Z, Shao Q, Xue C. GSDMD-mediated pyroptosis: a critical mechanism of diabetic nephropathy. *EXPERT REV MOL MED*. 2021;23:e23.
39. Xu S, Wang J, Zhong J, Shao M, Jiang J, Song J, Zhu W, Zhang F, Xu H, Xu G, et al. CD73 alleviates GSDMD-mediated microglia pyroptosis in spinal cord injury through PI3K/AKT/Foxo1 signaling. *CLIN TRANSL MED*. 2021;11(1):e269.
40. Correia DSM, Gjorgjieva M, Dolicka D, Sobolewski C, Foti M. Deciphering miRNAs' Action through miRNA Editing. *INT J MOL SCI* 2019, 20(24).
41. Zhu J, Liu B, Wang Z, Wang D, Ni H, Zhang L, Wang Y. Exosomes from nicotine-stimulated macrophages accelerate atherosclerosis through miR-21-3p/PTEN-mediated VSMC migration and proliferation. *THERANOSTICS*. 2019;9(23):6901–19.
42. Guo J, Mei H, Sheng Z, Meng Q, Veniant MM, Yin H. Hsa-miRNA-23a-3p promotes atherogenesis in a novel mouse model of atherosclerosis. *J LIPID RES*. 2020;61(12):1764–75.
43. Zhang F, Zhang R, Zhang X, Wu Y, Li X, Zhang S, Hou W, Ding Y, Tian J, Sun L, et al. Comprehensive analysis of circRNA expression pattern and circRNA-miRNA-mRNA network in the pathogenesis of atherosclerosis in rabbits. *Aging*. 2018;10(9):2266–83.
44. Zhang S, Song G, Yuan J, Qiao S, Xu S, Si Z, Yang Y, Xu X, Wang A. Circular RNA circ_0003204 inhibits proliferation, migration and tube formation of endothelial cell in atherosclerosis via miR-370-3p/TGFbetaR2/phosph-SMAD3 axis. *J BIOMED SCI*. 2020;27(1):11.
45. Sun L, Ma W, Gao W, Xing Y, Chen L, Xia Z, Zhang Z, Dai Z. Propofol directly induces caspase-1-dependent macrophage pyroptosis through the NLRP3-ASC inflammasome. *CELL DEATH DIS*. 2019;10(8):542.

Publisher's note

Springer Nature remains neutral with regard to jurisdictional claims in published maps and institutional affiliations.